Directing Osteogenesis of Stem Cells with Drug-Laden, Polymer-Microsphere-Based Micropatterns Generated by Teflon Microfluidic Chips

Xuetao Shi, Song Chen, Jianhua Zhou, Haijun Yu, Lei Li, and Hongkai Wu**

Human bone tissue is built in a hierarchical way by assembling various cells of specific functions; the behaviors of these cells in vivo are sophisticatedly regulated. However, the cells in an injured bone caused by tumor or other bone-related diseases cannot properly perform self-regulation behaviors, such as specialized differentiation. To address this challenge, a simple one-step strategy for patterning drug-laden poly(lactic-*co*-glycolic acid) (PLGA) microspheres into grooves by Teflon chips is developed to direct cellular alignment and osteogenic commitment of adipose-derived stem cells (ADSCs) for bone regeneration. A hydrophilic model protein and a hydrophobic model drug are encapsulated into microsphere-based grooved micropatterns to investigate the release of the molecules from the PLGA matrix. Both types of molecules show a sustained release with a small initial burst during the first couple of days. Osteogenic differentiated factors are also encapsulated in the micropatterns and the effect of these factors on inducing the osteogenic differentiation of ADSCs is studied. The ADSCs on the drug-laden micropatterns show stronger osteogenic commitment in culture than those on flat PLGA film or on drug-free grooved micropatterns cultured under the same conditions. The results demonstrate that a combination of chemical and topographical cues is more effective to direct the osteogenic commitment of stem cells than either is alone. The microsphere-based groove micropatterns show potential for stem cell research and bone regenerative therapies.

1. Introduction

Human bone tissue is built in a hierarchical and exquisite way by assembling various cells (osteoblasts, osteoclasts and osteocytes) of specific functions; the behaviors of these well-organized cells in vivo, including the proliferation, differentiation, apoptosis, arrangement and protein secretion of cells, are sophisticatedly managed.[1,2] In healthy bone tissue, organized osteoblasts produce a matrix of osteoid composed mainly of mineralized collagenous fibers with self-organized longitudinal and transversal orientations, which is considered to be one of the vital factors responsible for the anisotropic mechanical properties of bone.[3–5] However, different from the cells in a healthy human body, the cells in an injured bone caused by tumor or other bone-related diseases cannot perform self-regulated behaviors properly such as the specialized differentiation. In these cases, tissue-engineering strategies that effectively coordinate and direct cell behaviors for bone tissue repair is crucial to address the aforementioned issue.

Currently, there are two main approaches for directing cell behaviors in tissue engineering of bones, i.e., chemical/biological signal cues and topographical cues. The chemical/biological signal stimulation has been demonstrated to be effective to regulate cell behaviors, especially to direct cell differentiation.[6–8] Human stem cells have the potential to differentiate into diverse specialized cell types and have excellent self-renewable property, and thus become an overwhelmingly favorable choice for cell-based regenerative therapies. However, implanting undifferentiated stem cells into injured tissues might result in an adverse and undesired outcome, for example, in the condition of cartilage regeneration, bone spurs are formed instead.[9] Hence, the chemical/biological signal stimulation has drawn ever-growing interest in regulating stem cell differentiation towards a specialized cell lineage. Numerous growth factors and chemical reagents have been utilized to induce the specialized commitments of various stem cells.[10,11] Besides growth factors that have effect on the induction and promotion of osteogenic commitment of stem cells, some chemical reagents such as dexamethasone (Dex), ascorbic acid (ASC) and β-glycerophosphate (GP), the key osteogenic factors in cell culture media for osteogenesis, have also been loaded into scaffolds to induce cell differentiation due to their longer active half-life and higher stability.[12–17] The superiorities of these chemicals will prolong the interaction period between stem cells and chemical molecules released from the

Dr. X. T. Shi, Dr. S. Chen, Dr. J. H. Zhou,
Dr. H. J. Yu, Dr. L. Li, Prof. H. K. Wu
WPI-Advanced Institute for Materials Research
Tohoku University
Sendai 980-8578, Japan
E-mail: shi-xt@hotmail.com; chhkwu@ust.hk
Dr. J. H. Zhou, Prof. H. K. Wu
Department of Chemistry
Hong Kong University of Science and Technology
Hong Kong, China
Dr. L. Li
State Key Laboratory of Integrated Optoelectronics
Institute of Semiconductors
Chinese Academy of Sciences, Beijing, 100083, China

DOI: 10.1002/adfm.201200914

scaffolds. Several studies have also revealed that approaches using chemicals or biomolecules to stimulate cells displayed a remarkable effect on the induction of stem cell towards specialized differentiation.[12–14,17–20] Although chemicals and biomolecules are very effective in inducing stem cell differentiation, one major challenge of this method is that chemicals alone are difficult to control cell spatial arrangements such as cell alignments.

Different from chemical cue, topographical cue is often used to guide cells to orientate, which is important in bone development. By taking advantage of micro/nanopatterning techniques that have been developed in the past decades, flat surfaces (and certain curved surfaces) can be patterned with arbitrary features with sizes down to the nanometer range.[21–27] In this approach, guided by the surface topographical morphologies of pre-patterned scaffolds, cells and their produced extracellular matrix can be assembled into diversely exquisite morphologies resembling the microscopic structures of different tissues.[28–34] The micropatterned scaffolds have been widely used to direct cell arrangement and even to construct various tissues due to their benign characteristics in promoting cell response by inducing morphological and biological changes. For example, hydrogel-based micropatterns have been developed to guide cell organization and alignment for bone repair.[35,36] Aubin et al.[37] have fabricated microengineered gelatin hydrogels to direct cellular alignment and microconstruct potential muscle tissue. Although cell orientation and cell morphology can be regulated using the scaffolds with micro/nanopatterned topographical cues, this approach is less effective in directing the differentiation of stem cells into specialized cells. Providing that a scaffold combining desired topographic morphology and the characteristics of well encapsulation and controlled-release of cellular differentiated factors is explored, the orientation and differentiation of stem cells that facilitate bone tissue regeneration in a biomimetic manner could be managed simultaneously.

We combine the two approaches to simultaneously regulate the differentiation of stem cells and cell orientation by encapsulating osteogenic differentiation factors into micropatterned ploy(lactic-*co*-glycolic acid) (PLGA) grooves. PLGA has recently become a prevalent choice for the study of in vitro bone regeneration and development because it is biocompatible and biodegradable, and the release of various encapsulated substances (e.g., hydrophilic and hydrophobic drugs,[38] growth factors,[39] protein,[40] and SiRNA[41]) in PLGA can be well regulated. Although PLGA has been studied widely, it is non-trivial to micropattern this material with active drug loaded. Current micropatterning techniques such as inkjet printing and laser interference lithography are restricted to certain materials with particular properties; moreover, complicated procedures and expensive equipment are required. Similarly, soft lithographic techniques that utilize polydimethylsiloxane (PDMS) to transfer desired micropatterns to different materials are unsuitable for the generation of PLGA micropatterns because of the weak resistance of PDMS to organic solvents (e.g., methylene chloride for PLGA preparation) and the possible loss of critical molecules to the bulk and surface of PDMS during pattern formation. To overcome the difficulties, we use Teflon molding technique to transfer micropatterns into PLGA. Compared with PDMS, Teflon is endowed with some unique characteristics that are beneficial to our purpose here. Teflon virtually sticks to almost nothing; it also shows strong resistance to all organic solvents and has excellent heat stability.[42,43] These superiorities facilitate the formation of PLGA micropatterns and support the encapsulation of drug/protein into PLGA matrix.

Here, we used hydrophilic fluorescein isothiocyanate labelled bovine serum albumin (FITC-BSA) and hydrophobic fluorescein labelled Dex as the model molecules to demonstrate the encapsulation of different types of molecules into PLGA

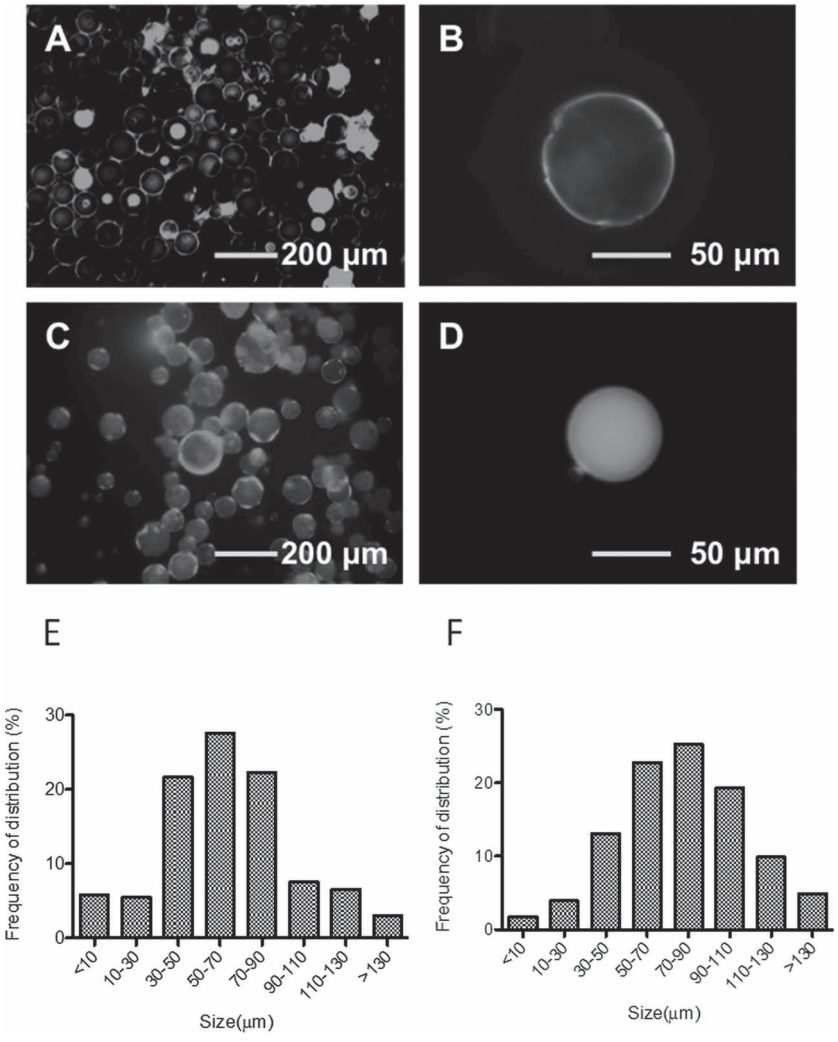

Figure 1. Fluorescence images and typical particle sizes distribution of hydrophilic FITC-BSA (A,B,E) and hydrophobic fluorescein Dex (C,D,F) laden PLGA microspheres.

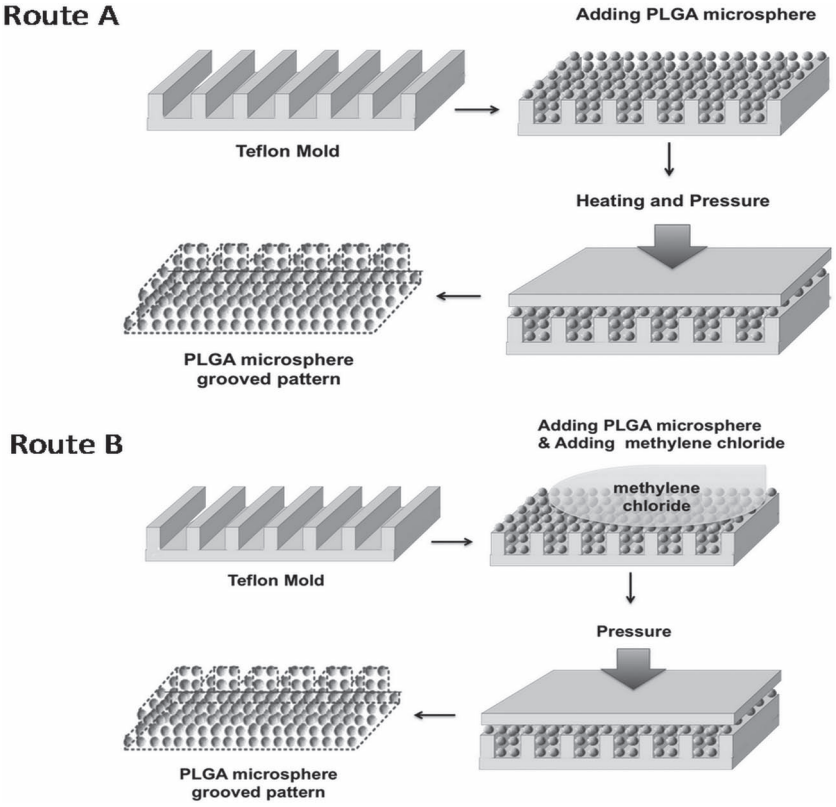

Figure 2. Schematic illustrations showing two routes for fabricating PMGMs. In Route A, PMGMs were prepared by heating treatment; In Route B, PMGMs were prepared by solvent fusion.

microspheres, which was subsequently used to generate micropatterned grooves. This newly established controlled release system (drug laden PLGA microspherebased grooved micropatterns) is abbreviated as "drug-laden PMGMs" system. We also encapsulated osteogenic differentiated factors, dexamethasone (Dex), ascorbic acid 2-phosphate (ASC), and β-glycerophosphate (GP), into the PLGA micropatterns and studied their ability to induce osteogenic commitment of stem cells. Adipose-derived stem cells (ADSCs) were cultured onto these drug-laden PMGMs, and the osteogenic commitment of ADSCs induced by the combined effects of chemicals and topography was investigated.

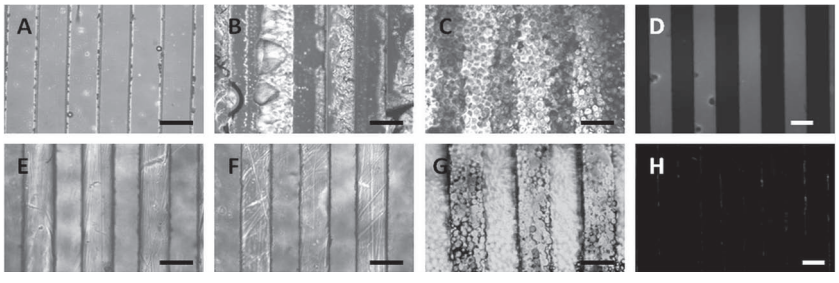

Figure 3. Images of PDMS (A) and Teflon chips (E). The PDMS stamp after the treatment of methylene chloride (B), the Teflon chip after the treatment of methylene chloride (F), PMGMs generated by a PDMS stamp (C), and by a Teflon chip (G). Fluorescence images of the PDMS stamp (D) and the Teflon chip (H) after being soaked in a FITC-BSA solution for 2 h. (Scale bars, 200 μm).

2. Results and Discussion

2.1. Preparation of Drug-Laden PMGM

Before being printed, hydrophobic and hydrophilic drug/protein-laden PLGA microspheres were prepared using single emulsion and double emulsion techniques, respectively. Fluorescence labeled BSA and Dex were used as the hydrophilic and hydrophobic model drug/protein, respectively. Both types of microspheres were loaded with the same amount of fluorescence labeled drugs or proteins (2 mg drug or protein/1.5 g PLGA). The encapsulation efficiencies of BSA and Dex in PLGA microspheres were 29.5% ± 3.9% and 55.6% ± 7.9%, respectively. As shown in **Figure 1**, the distribution of Dex in PLGA microspheres (Figure 1C,D) is more uniform than that of BSA (Figure 1A,B). The main reason of different encapsulation efficiencies and distributions of Dex and BSA in PLGA microspheres was attributed to the different ways of microspherical preparation. The microspherical size distribution of BSA-laden and Dex-laden microspheres is shown in Figure 1E,F; most particles have the size ranging from 30 μm to 90 μm for BSA-laden microspheres, and from 30 μm to 130 μm for Dex-laden microspheres. The average size of BSA-laden microspheres and Dex-laden microspheres are 67.7 μm ± 66.3 μm and 70.2 μm ± 68.5 μm, respectively.

The processes for the generation of PLGA micropatterns are shown in **Figure 2**. A pre-designed Teflon chip was prepared, and then the pre-prepared PLGA microspheres were placed onto the Teflon chip. Then a flat Teflon slide was covered onto the Teflon chip under pressure and heating (Route A) to form a PMGM. Nevertheless, this routine for preparation of protein-laden PMGM is not feasible. It is well known that one major challenge in designing protein-laden vehicles is to maintain the stability and bioactivity of the encapsulated proteins. In Route A, high temperature, which often induces protein denaturation, was required to stick the dispersed PLGA microspheres together. Therefore, in order to maintain the bioactivity of encapsulated protein, a solvent fusion method is adopted instead. As shown in the second step of Route B, methylene chloride was added onto the Teflon chip to fuse PLGA microspheres into a grooved micropattern.

Here, we used a Teflon chip (**Figure 3**E) to transfer the grooved micropatterns instead of conventional PDMS (Figure 3A) due to the following reasons. First, the PDMS stamp is highly elastic with a Young's modulus of 1 MPa. In the third step of both Route A and B (Figure 2), providing that PDMS stamp was used to replace the Teflon chip, the original

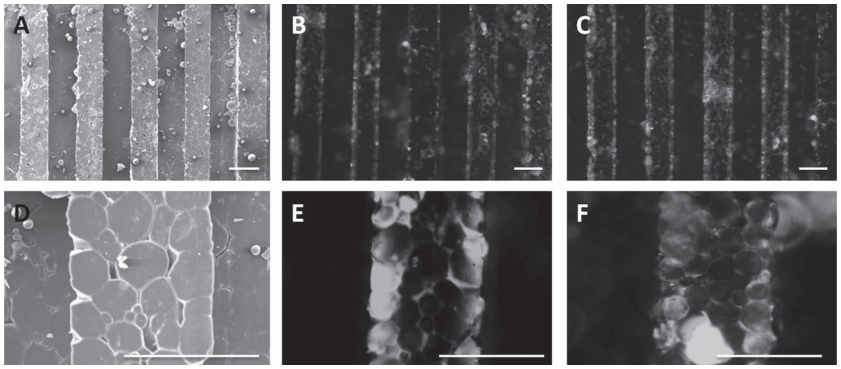

Figure 4. Scanning electron microscopy (SEM) images of PMGMs (A,D), and fluorescence images of FITC-BSA (B,E) and fluorescein Dex (C,F) laden PMGMs. Scale bars are 200 μm.

patterns on elastomeric PDMS stamp will be distorted after being transferred to PLGA matrix under pressure. However, the Teflon chip with a Young's modulus of 500 MPa is significantly tougher than PDMS, so the patterns transferred from the Teflon chip will have mild distortion under pressure. Secondly, when we produced protein-laden PMGMs, the organic solvent, methylene chloride was used. PDMS has weak resistance to this harsh organic solvent (Figure 3B), and thus cannot produce desired PMGMs according to the PDMS stamp (Figure 3C). Contrarily, Teflon can resist to almost all organic solvents. Therefore, after contacting with organic solvent, the Teflon chip still maintains the well-arranged microstructure pattern (Figure 3F), and facilitates to the achievement of desired PMGMs (Figure 3G). Thirdly, PDMS strongly adsorbs biomolecules on its surface (Figure 3D). Owing to this property, PDMS stamp will influence the drug/protein encapsulation efficiencies of the drug/protein-laden PMGMs. In contrast, Teflon virtually sticks to almost nothing on its surface (Figure 3H), which will benefit the loading of drug/protein-laden into PLGA matrix instead of the surface of stamp. Taken together, Teflon is more suitable than PDMS for the preparation of drug/protein-laden PMGMs.

The morphologies of FITC-BSA laden and fluorescein Dex-laden PMGMs are shown in **Figure 4**. The grooved micropattern built by microspheres is with well-arranged morphology. It is also observed that microspheres were deformed attributed to heat and pressure in Route A, or solvent in Route B. Although the microspheres were deformed, the drug/protein encapsulation efficiencies were not significantly influenced. The encapsulation efficiencies of BSA (27.9% ± 2.5%)and Dex (51.2% ± 3.6%) in PMGMs show no significant change when compared with the encapsulation efficiencies of BSA protein (29.5% ± 3.9%) and Dex in PLGA microspheres (55.6% ± 7.9%).

2.2. Drug/Protein Release

We used BSA and Dex as the hydrophilic and hydrophobic model drugs, respectively; and loaded them into PLGA microspheres, which subsequently formed the grooved micropatterns. Figure S1A,B (Supporting Information) shows the normalized release profiles of BSA and Dex from the drug/protein-laden PMGMs. The release at each time point was normalized to the final drug/protein loading in the micropatterns. Both profiles exhibit an exponential release tendency. During the initial burst (from day 0 to day 5), the respective protein/drug release for BSA-laden and Dex-laden PMGMs was around 45% and 35% of the total protein/drug loading amount. Up to 20 days, the total protein/drug release from both BSA-laden and Dex-laden PMGMs were more than 70%. The fluorescence images of FITC-BSA laden and fluorescein Dex-laden PMGMs after undergoing incubation in PBS solution for 2 weeks are shown in Figure S1C,D (Supporting Information). The fluorescence produced by the residual protein and drug molecules in the PMGMs can still be observed after 2 weeks of release. The fluorescence intensity of fluorescein Dex is significantly stronger than that of FITC-BSA, indicating higher drug/protein encapsulation efficency and slower drug/protein release rate. Compared with other biomaterials such as hydrogels using for micropatterning, PLGA has the ability to release both hydrophilic and hydrophobic molecules with the release time of many days. In contrast, most of the hydrogels can only encapsulate and release hydrophilic molecules, and the release period just last for hours.

In order to induce osteogenic differentiation of stem cells, multi-drug-laden PMGMs were prepared, in which the hydrophilic drugs, ASC and GP, and hydrophobic drug, Dex were loaded simultaneously. The multi-drug-laden microspheres were prepared via a typical double emulsion technique. First, ASC and GP were dissolved into an aqueous phase, and then emulsified into Dex-PLGA composite solution, and subsequently emulsified in an aqueous solution for 12 h to harden the formed microspheres. The multi-drug-laden PMGM was generated using the similar method to prepare BSA/Dex-laden PMGMs. As indicated in **Figure 5**, all the release profiles for the same molecules exhibit similar trend. The hydrophilic drugs, ASC and GP showed fast release for the first 5 days. More than 80% and 70% of the respective total loading amount of ASC and GP were released from the drug-laden PMGMs. Up to 20 days, the total ASC and GP release from the PMGMs had reached nearly 100%, in which the release rate of GP was slower than that of ASC. The profiles of Dex release from the micropatterns for 20 days are also shown in Figure 5. The release curves of Dex exhibited similar trends of that of Dex-laden PMGM (Figure S1B, Supporting Information), and low initial burst release among the three encapsulated drugs due to its hydrophobicity. We also found that drug-laden PMGM with either wide grooves (200 μm) or narrow grooves (50 μm) and drug-laden microsphere- based flat film without patterning exhibited almost no significant differences on all of the release of drugs.

2.3. Cellular Alignment and Differentiation

ADSCs were cultured on the Dex-ASC-GP laden PMGMs for 14 days. To observe the cell morphology and proliferation, cells were stained with phalloidin for F-actin and DAPI for nuclei. The cellular alignment was quantitatively determined by the alignment angles of their nuclei. The cells are considered to be well aligned if the angle of the nuclear alignment is between 0°

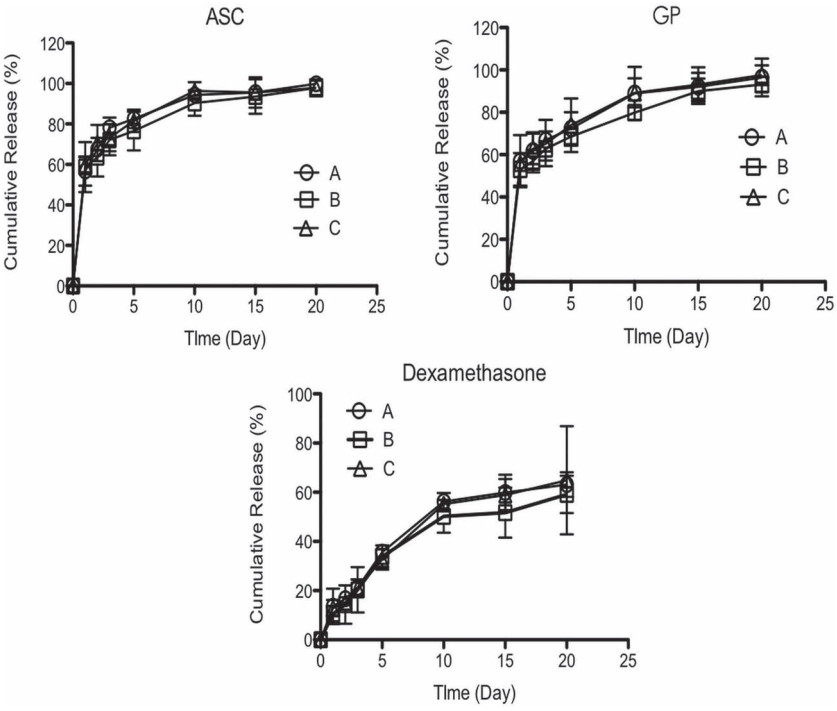

Figure 5. Cumulative release profiles of ASC, GP, and Dex from PMGMs with wide (200 μm, A) and narrow (50 μm, B) grooves as well as from PLGA microsphere-based flat films (C).

to 10°. As shown in **Figure 6** and **Figure 7**, most of the cells were aggregated into grooves of the PMGMs, and showed aligned structures. In contrast, cells cultured on non-patterned PLGA microsphere-based flat films exhibited no obvious alignment. More than 40% cells grown on the drug-laden PMGMs with narrow grooves (50 μm) were aligned with the groove direction while only ≈10% cells on the PLGA microsphere-based flat films were (Figure 7D). The aligned cell number on drug-laden PMGMs with wide grooves (200 μm) was half of that on the drug-laden PMGMs with narrow grooves, and two folds of that on the PLGA microsphere-based flat films. The result is consistent with the observation of the alignment of nuclei after being stained by DAPI (Figure 7A–C). As shown in Figure 7A–C,E–J, the alignment of nuclei as well as F-actin on drug-laden PMGMs with narrow grooves (50 μm) can be clearly seen, while there are only a very small portion of cells with aligned nuclei and F-actin for PMGMs with wide groves (200 μm). The cells cultured on PLGA microsphere-based flat films showed random arrangement of nuclei and F-actin. The results clearly demonstrate that cell alignment can be effectively directed by the morphologies of PMGMs.

This control of cell alignment can be used to regulate cell phenotypes and functions. Numerous studies have been conducted to investigate the effect of cell alignment on cell proliferation and differentiation.[44–47] The alignment of electrospun poly-L-lactic acid (PLLA) fibers can promote the migration of endothelial cells and benefit the reconstruction of lymphatic vessels.[48] Three-dimensional hydrogels with alignment microstructure were developed to direct the cellular alignment and elongation of myoblasts.[37] For bone tissue engineering, the alignment of cell can promote the construction of biomimetic bone microstructure that is composed by orientated mineralized collagenous fibers (which is important for high bone strength). Mesenchymal stem cells (MSCs) cultured on TiO_2 nanotubes showed an aligned and elongated morphology, which indicated the selective differentiation of MSCs into osteoblastic-like cells.[49] Therefore, it might be possible to induce stem cells towards osteogenic differentiation in situ by controlling cell alignment under the steering of the grooved micropatterns.

Herein, the Dex-ASC-GP multi-drug-laden PMGMs were used to induce cellular alignment and osteogenic commitment of ADSCs in situ. Ten thousands of cells were seeded onto the micropatterns, and around 50% cells were attached onto the micropatterns. The same amount of cells cultured on the drug-laden PLGA microsphere-based flat film and drug free PLGA microsphere-based flat film was used as controls. The osteogenic phenotype of cells on drug-laden PMGMs was further studied to confirm the resulting osteogenic differentiation. As shown in **Figure 8**, after 14 days

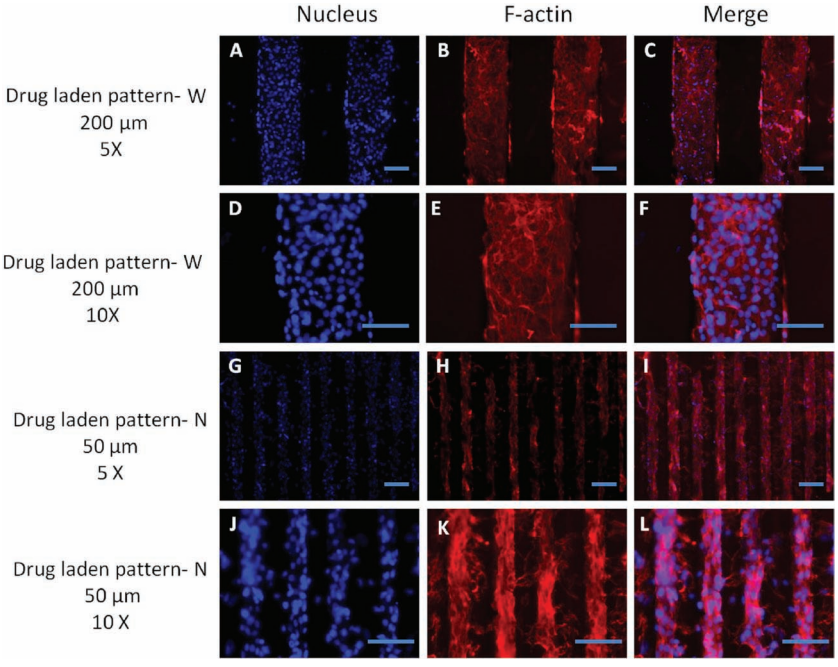

Figure 6. Nuclear and F-actin staining of ADSCs on ASC-GP-Dex laden PMGMs with wide (W, 200 μm) and narrow (N, 50 μm) grooves after 14 days of culture. Scale bars are 200 μm.

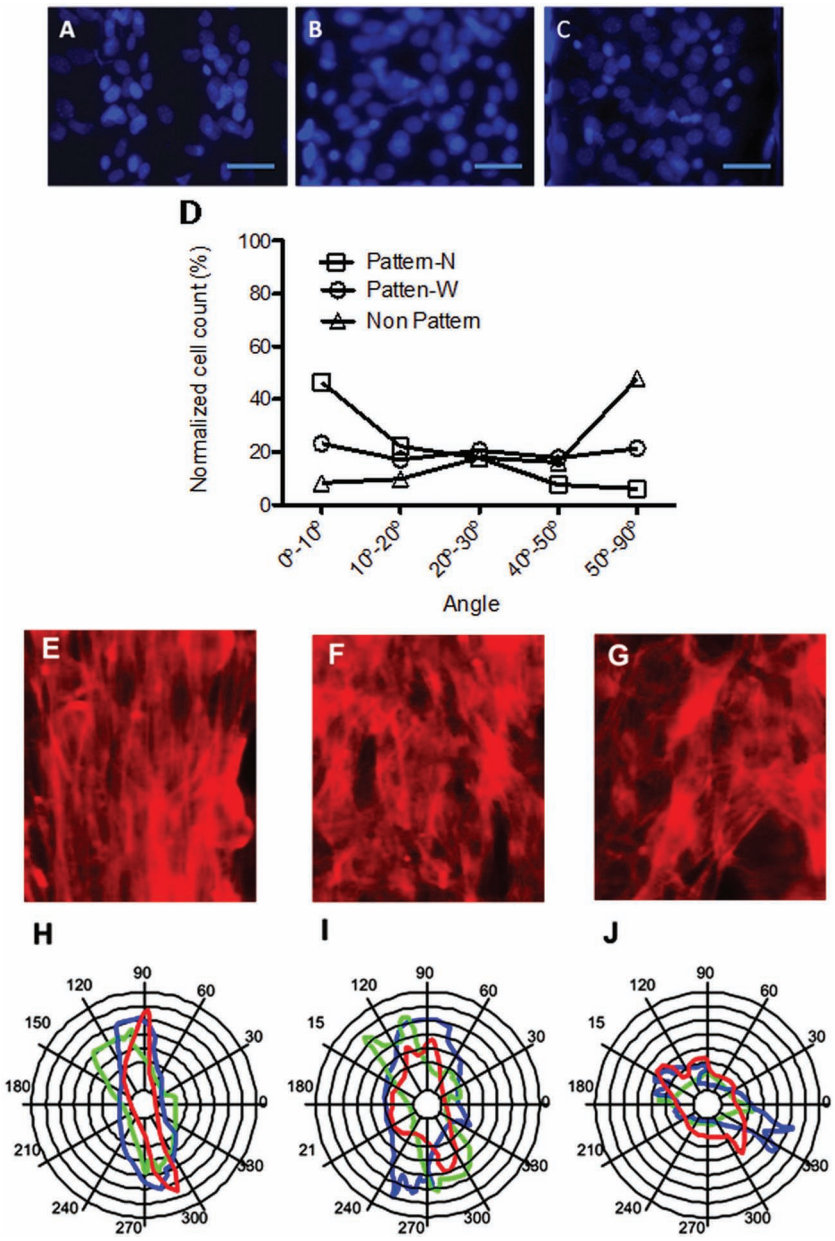

Figure 7. Alignment of nuclear and F-actin of ADSCs on ASC-GP-Dex laden PMGMs with narrow (N, 50 μm), wide (W, 200 μm) grooves, and microsphere-based flat film (control) after 14 days of culture. Scale bars are 50 μm. A–C) Nuclear staining of ADSCs on ASC-GP-Dex laden PMGMs with narrow (N, 50 μm), wide (W, 200 μm) grooves, and PLGA flat film (control), respectively. D) aligned cell nuclei counting. E–G) F-actin staining of ADSCs on ASC-GP-Dex laden PMGMs with narrow (N, 50 μm), wide (W, 200 μm) grooves, and microsphere-based flat film (control), respectively. H–J) Polar plots revealing the orientation distribution of F-actin for ADSCs on ASC-GP-Dex laden PMGMs with narrow (N, 50 μm), wide (W, 200 μm) grooves and PLGA microsphere-based flat film (control), respectively. Each plot is an average of six replicates; 90° and 270° represent the direction of grooves.

of culture, the activity of alkaline phosphatase (ALP, which is an early marker for osteogenesis and an important enzyme produced by osteoblasts) and the secretion of osteocalcin (which is a late osteogenic marker and a main noncollagenous protein associated with the formation of mineralized matrix of bone) in ADSCs cultured on drug-laden PMGMs were quantitatively determined. The activity of ALP and the secretion of osteocalcin in ADSCs cultured on drug-laden samples were at least 4-fold higher than those cells on drug- free samples. Among the drug-laden groups, cells on drug-laden PMGMs with narrow grooves (50 μm) exhibited significantly higher ALP activity than both cells on drug-laden PMGMs with wide grooves (200 μm) and cells on drug-laden microsphere-based flat film. The secretion of collagen was also studied in this work because it is a major constitute of bone matrix. After 14 days of culture, the secretion of collagen in ADSCs cultured on drug-laden narrow and wide grooves has no significant difference, while cells on these drug-laden PMGMs showed significant higher collagen secretion than those cultured on drug-laden microsphere-based flat film. Although the expression of osteogenic markers for ADSCs on drug-free groups was lower when compared with drug-laden groups, the cells on drug-free PMGMs with narrow grooves still showed higher expression of ALP, collagen and osteocalcin when compared with those on drug-free PMGMs with wide grooves and on drug-free microsphere-based flat film. The up-regulated expression of these three important proteins in ADSCs cultured on drug-laden PMGMs with narrow grooves indicates enhanced induction of ADSCs towards osteoblastic cells.

It is well known that ADSCs have the capacity to self-renew and differentiate into different cell lineages such as myocytes, osteoblasts, chondrocytes and adipocytes. Some studies have reported that cellular alignment enhanced cell growth or phenotypes and directed stem cell towards a specialized cell type.[50–54] We found that cell alignment alone is less effective to induce osteogenic differentiation of stem cells (Figure 8). Moreover, although the chemical or biological stimulations such as the treatment of cells with growth factors or cell-differentiated factors play a critical role in cell differentiation, ADSCs showed better osteogenic differentiation with the assistance of grooved micropatterns, which induces cellular alignment (Figure 8). Therefore, the collaboration of topographical and chemical/biological cues promote better osteogenic commitment of ADSCs when compared with an individual chemical or physical stimulation.

3. Conclusion

We present a simple, one-step method for generating drug/protein-laden PMGMs by Teflon chips to direct osteogenesis of stem cells. The micropatterns exhibit excellent release of

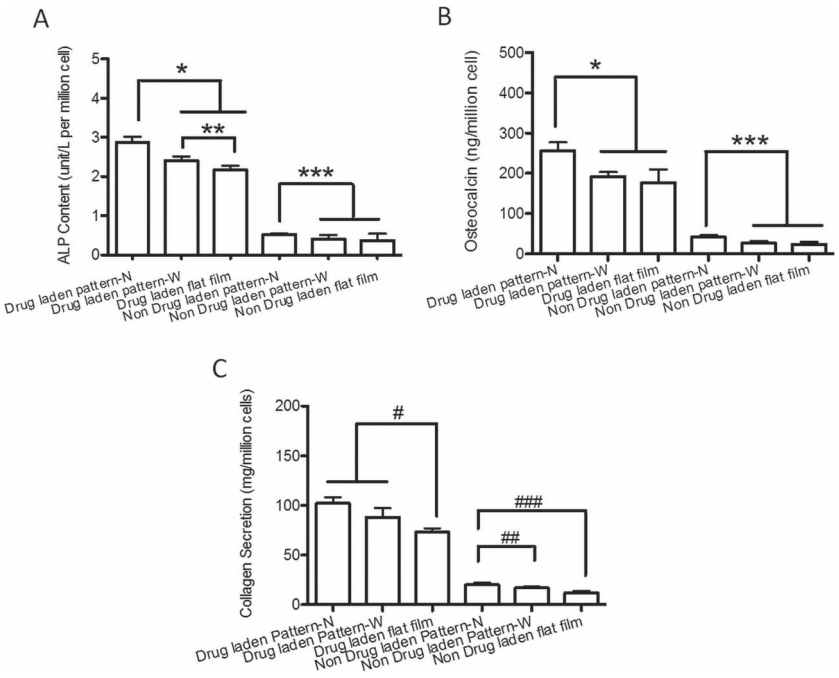

Figure 8. Expression of ALP activity (A), osteocalcin (B), and collagen (C) of ADSCs on ASC-GP-Dex laden PMGMs with wide (W, 200 μm) and narrow (N, 50 μm) grooves after 14 days of cell culture. ADSCs cultured on drug-laden and drug-free microsphere-based flat films, and drug-free PMGMs with wide (W, 200 μm) and narrow (N, 50 μm) grooves were used as controls. *, **, and *** indicate statistical significance when compared with cells cultured on drug-laden PMGMs with wide grooves and drug-laden PMGMs with narrow grooves, drug-laden microsphere-based flat films, and drug-free PMGMs with wide grooves and drug-free microsphere-based flat film ($p < 0.05$), respectively. #, ##, and ### indicate statistical significance when compared with cells cultured drug laden flat films, drug-free PMGMs with wide grooves, and drug-free microsphere-based flat films.

both hydrophilic model protein, BSA and hydrophobic model drug, Dex. In order to induce the osteogenic differentiation of ADSCs, cell differentiated factors (Dex, ASC and GP) were loaded into PMGMs. After cultured on these multi-drug-laden PMGMs for 14 days, ADSCs showed stronger osteogenic commitment when compared with the cells cultured on drug-laden PLGA microsphere-based flat film and drug-free PMGMs. The combination of cellular alignment and the release of osteogenic differentiated factors promote the osteogenic commitment of ADSCs better when compared with an individual stimulation alone. In summary, this novel micropatterning technique should have great potential for stem cell research and stem cell based bone tissue regeneration.

4. Experimental Section

Preparation of Teflon Chip: The teflon chip was fabricated according to a previously described method.[42,43] Briefly, a thin PDMS (GE, China) master was molded from photoresist microstructures produced with standard photolithography, and then sealed to a glass slide. A Teflon plate (≈1.0 mm thick, Yuyisong Inc., China) was sandwiched between the PDMS master and another flat glass slide. The sandwich assembly was placed on a hot compressor (TM-101F, Taiming, Inc., US), embossed at 275 °C for 5 min, and then cooled to room temperature. The teflon chip was obtained after removing both the PDMS master and glass slide.

Preparation of BSA/FITC-BSA Laden PLGA Microspheres: BSA-laden/FITC-BSA-laden PLGA microspheres were prepared by a double emulsion method.[55] Briefly, 2 mg BSA (Sigma-Aldrich, US) or FITC-BSA (Sigma-Aldrich, US) was dissolved in 1 mL PBS solution to form the first aqueous phase W_1. The organic phase (O) was prepared by dissolving 1.5 g PLGA (Mw ≈ 10 000, Wako, Japan) into 15 mL methylene chloride. The BSA/FITC-BSA solution was then emulsified in PLGA solution at 1200 rpm for 15 min to form the primary W_1/O. The W_1/O emulsion was promptly added into 500 mL 0.1% polyvinyl alcohol (PVA, Mowiol 4-98, Mw ≈ 27 000, Sigma-Aldrich, US) aqueous solution. The resulting $W_1/O/W_2$ emulsion was stirred at 750 rpm for 12 h at room temperature to evaporate the organic solvent and to solidify the protein-laden microspheres. The microspheres were finally washed three times with deionized water. Drug-free PLGA microspheres were prepared using the similar method without the addition of BSA or FITC-BSA into PLGA solution.

Preparation of Dex-Laden/Fluorescein Dex-Laden PLGA Microspheres: Dex-laden/Fluorescein Dex-laden PLGA microspheres were prepared by a single emulsion method.[56] Briefly, 1.5 g PLGA was dissolved in 15 mL methylene chloride containing 2 mg Dex (Sigma-Aldrich, US) or 2 mg fluorescein Dex (Invitrogen, US). The mixture was poured into 500 mL 0.1% PVA aqueous solution and stirred at 750 rpm for 12 h. The resulting PLGA microspheres were isolated, and washed three times with deionized water.

Preparation of GP-ASC-Dex Laden PLGA Microspheres: *GP-ASC-Dex* laden PLGA microspheres were prepared by a double emulsion method. Briefly, 500 mg GP (Sigma-Aldrich, US) and 150 mg ASC (Wako, Japan) was dissolved in 2 mL PBS solution to form the first aqueous phase W_1. The organic phase (O) was prepared by dissolving 1.5 g PLGA and 2 mg Dex (Mw~10,000, Wako, Japan) into 15 mL methylene chloride. The GP solution was then emulsified in PLGA solution at 1200 rpm for 15 min to form the primary W_1/O. The W_1/O emulsion was promptly added into 500 mL 0.1% PVA aqueous solution. The resulting $W_1/O/W_2$ emulsion was stirred at 750 rpm for 12 h at room temperature to evaporate the organic solvent and to solidify the drug-laden microspheres. The microspheres were finally washed three times with deionized water.

Particle Size Distribution of PLGA Microspheres: The size distribution of fluorescein Dex or FITC-BSA laden PLGA microspheres was analyzed with a fluorescence microscope (Zeiss, Germany) by randomly selecting 300 microspheres from a total of 15 visual fields. The frequency (%) of diameters was recorded in increments of 20 μm.

Preparation of PMGMs: PMGMs and drug-laden PMGMs were prepared via two different routes (Figure 2). Briefly, 100 mg of protein/drug-laden PLGA microspheres was added onto the Teflon chip, and then covered by a Teflon film. For drug-laden microspheres (Route A), the sandwich assembly was placed on a hot compressor (TM-101F, Taiming, Inc., US), embossed for 10 s at 80 °C, and cooled down to room temperature. For protein-laden microspheres (Route B), methylene chloride was added onto the Teflon mold after the protein laden PLGA microspheres were laden, and then the Teflon mold was covered with a flat Teflon slide. Subsequently, the sandwiched sample was washed with deionized water to remove redundant organic solvent until the microspheres were fully fused. The morphologies of the FITC-BSA and fluorescein Dex laden PMGMs were observed using a fluorescence microscope (Zeiss, Germany). Non- patterned PLGA microsphere-based flat film was prepared using the same method. Another flat Teflon film was used to replace the grooved Teflon chip.

Drug/Protein Release: The release of Dex/BSA/GP/ASC from PMGMs was determined by suspending drug-laden PMGMs in 0.9 M NaCl solutions. The media of samples were collected periodically with equal amount of NaCl solution. The concentrations of released Dex was measured at the maximum absorbance wavelength of Dex (242 nm), BSA was measured using QuantiProBCA assay kit (BSA, Sigma-Aldrich, US), and GP/ASC were measured using PiPer Phosphate Assay Kit (GP&ASC, Invitrogen, US). The percentage of cumulative released was obtained by normalizing the released amount to the total amount loaded into PMGMs. To examine the release of fluorescein Dex or FITC-BSA from PMGMs, fluorescein Dex/FITC-BSA laden PMGMs were incubated in 2.0 mL PBS solution. After 2 weeks, the micropatterns were observed using a fluorescence microscope (Zeiss, Germany).

Cell Culture and Seeding: Adipose-derived stem cells (Human's ADSC, DS Pharm Biomedical Inc., Japan) were propagated in Dulbecco's modified Eagle's medium (DMEM)/F12 supplemented with 10% (v/v) fetal bovine serum (FBS, Invitrogen, US), 1% penicillin/streptomycin (Invitrogen, US), and were maintained in an incubator. Dex-ASC-GP laden PMGMs were placed in cell culture dishes and sterilized under UV light for 30 min. 200 µL of fibroblasts suspension (5×10^5 cells/mL) were loaded onto each micropattern (2 cm × 2 cm) and then was incubated in an incubator. After 1 day of culture, the media were replaced to remove non-adherent cells, and the media was subsequently replaced every three days.

Cellular Alignment: After 14 days of culture, the cells on Dex-ASC-GP laden PMGMs were fixed with 1% paraformaldehyde for 15 min and then with 0.1% Triton-X 100 (Sigma-Aldrich, US) for 5 min, the cells laden PMGMs were stained with DAPI (Invitrogen, US) and TRITC-phalloidin (Alexa-Fluor 594, Invitrogen, US) for 30 min to visualize cell nuclei and F-actin under fluorescence microscope. Quantification of cellular alignment was performed using a technique as described in the reference.[37] Briefly, the angles between the main axis parallel with the grooves of PMGMs and the main axis of nuclei (was considered as ellipses) was measured using NIH image software from the images of nuclei staining. The nuclear angle of a single cell less than 10° is considered to be aligned.

Cell Differentiation: The osteogenesis of ADSCs was evaluated by ALP activity, osteocalcin protein assays and collagen content. ALP activity of ADSCs was conducted using pNPP assay (p-nitrophenyl phosphate liquid substrate, Sigma-Aldrich, US). Briefly, after 14 days of culture, cells growing on the patterns were lysed in 0.1% Triton X-100 solutions for 15 min in 4 °C.[57–59] Subsequently, pNPP was added into the lysate, followed by incubation at 37 °C for 30 min. The absorbance at 405 nm of the solution was measured using plate reader (BioTex, US). ALP activity was calculated using a formula provided by manufacturer after normalizing cell number. Osteocalcin levels of the cells on the patterns were tested using Osteocalcin direct ELISA kit (Invitrogen, US) according to manufacturer's instruction. Collagen content was measured via hydroxyproline quantification.[60] Briefly, the cells on the micropatterns were digested and then added into a 4 M guanidine-HCl solution in 0.05 M sodium acetate. After centrifugation, the supernatant was discarded and then the residue was added into 5 mL of 6 M HCl and 2 mL edible oil, followed by heating at 115 °C for 4 h; afterwards, the residue was respectively treated with chloramine-T solution, perchloric acid solution and paradime thylaminobenzaldehyde solution. The absorbance of the resulting solution at 560 nm was determined. Collagen quantification was calculated from a standard curve of hydroxyproline.

Statistical Analysis: Six replicates were performed for every assay and the results were expressed as means ± standard deviations. Statistical analysis was performed using the paired or unpaired Student's t-tests to compare two experimental groups and ANOVA followed by the Tukey's multiple comparison tests when more than two experimental groups were analyzed.

Supporting Information

Supporting Information is available from the Wiley Online Library or from the author.

Acknowledgements

The authors acknowledge the support of by WPI-Initiative funding from Japan Society for Promotion of Science and Ministry of Education, Culture, Sports, Science and Technology, Japan. L.L acknowledges National Natural Science Foundation of China (No. 61078074) and National Basic Research Program of China (No. 2011CB933102). H.K.W. acknowledges the support from Hong Kong RGC (GRF 604509 and GRF 605210). The authors also express gratitude to Dr. H. X. Chang for helpful revision and Y. Hou for access to the SEM.

Received: March 31, 2012
Revised: May 9, 2012
Published online: June 4, 2012

[1] B. M. Gumbiner, *Cell* **1996**, *84*, 345.
[2] M. D. Kofron, A. Griswold, S. G. Kumbar, K. Martin, X. Wen, C. T. Laurencin, *Adv. Funct. Mater.* **2009**, *19*, 1351.
[3] D. A. Wang, C. G. Williams, F. Yang, N. Cher, H. Lee, J. H. Elisseeff, *Tissue Eng.* **2005**, *11*, 201.
[4] S. C. Marks, S. N. Popoff, *Am. J. Anat.* **1988**, *183*, 1.
[5] M. M. Stevens, J. H. George, *Science* **2005**, *310*, 1135.
[6] G. A. Hudalla, W. L. Murphy, *Adv. Funct. Mater.* **2011**, *21*, 1754.
[7] J. S. Lee, A. J. W. Johnson, W. L. Murphy, *Adv. Mater.* **2010**, *22*, 5494.
[8] M. R. Urist, R. J. DeLange, G. A. Finerman, *Science* **1983**, *220*, 680.
[9] L. J. Brunet, J. A. McMahon, A. P. McMahon, R. M. Harland, *Science* **1998**, *280*, 1455.
[10] D. A. Wang, S. Varghese, B. Sharma, I. Strehin, S. Fermanian J. Gorham, H. D. Fairbrother, *Nat. Mater.* **2007**, *6*, 385.
[11] K. Su, T. T. Lau, W. Leong, Y. Gong, D. A. Wang, *Adv. Funct.Mater.* **2012**, *22*, 972.
[12] S. Zhang, H. Uludağ, *Pharm. Res.* **2005**, *26*, 1561.
[13] I. Kratchmarova, B. Blagoev, M. Haack-Sorensen, M. Kassem, M. Mann, *Science* **2005**, *308*, 1472.
[14] F. von Konch, C. Jaquiery, M. Kowalsky, S. Schaeren, C. Alabre, I. Martin, H. E. Rubash, A. S. Shanbhag, *Biomaterials* **2005**, *26*, 6941.
[15] D. W. Green, I. Leveque, D. Walsh, D. Howard, X. Yang, K. Patridge, S. Mann, R. O. C. Oreffo, *Adv. Funct. Mater.* **2005**, *15*, 917.
[16] X. Shi, Y. Wang, R. R. Varshney, L. Ren, F. Zhang, D. A. Wang, *Biomaterials* **2009**, *30*, 3996.
[17] S. Ding, P. G. Schultz, *Nat. Biotechnol.* **2004**, *22*, 833.
[18] X. Shi, Y. Wang, L. Ren, Y. Gong, D. A. Wang, *Pharm. Res.* **2009**, *26*, 422.
[19] X. Shi, Y. Wang, L. Ren, N. Zhao, Y. Gong, D. A. Wang, *Acta Biomater.* **2009**, *5*, 1697.
[20] F. Yang, C. G. Williams, D. A. Wang, H. Lee, P. N. Manson, J. H. Elisseeff. *Biomaterials* **2005**, *26*, 5991.
[21] H. Wu, T. W. Odom, G. M. Whitesides, *J. Am. Chem. Soc.* **2002**, *124*, 7288.
[22] D.-H. Kim, C.-H. Seo, K. Han, K. W. Kwon, A. Levchenko, K.-Y. Suh. *Adv. Funct. Mater.* **2009**, *19*, 1579.
[23] X. Jiang, Q. Xu, S. K. W. Dertinger, A. D. Stroock, T.-M. Fu, G. M. Whitesides, *Anal. Chem.* **2005**, *77*, 2338.
[24] B. Yuan, Y. Jin, Y. Sun, D. Wang, J. Sun, Z. Wang, W. Zhang, X. Jiang, *Adv. Mater.* **2012**, *24*, 890.
[25] X. Jiang, R. Ferrigno, M. Mrksich, G. M. Whitesides, *J. Am. Chem. Soc.* **2003**, *125*, 2366.
[26] B. Xu, F. Arias, S. T. Brittain, X.-M. Zhao, B. Grzybowski, S. Torquato, G. M. Whitesides, *Adv. Mater.* **1999**, *11*, 1186.
[27] N. L. Jeon, I. S. Choi, B. Xu, G. M. Whitesides, *Adv. Mater.* **1999**, *11*, 946.

[28] S. H. Lee, J. J. Moon, J. L. West, *Biomaterials* **2008**, *29*, 2962.
[29] K. Kushiro, S. Chang, A. R. Asthagiri, *Adv. Mater.* **2010**, *22*, 4516.
[30] Y. F. Ding, J. R. Sun, H. W. Ro, Z. Wang, J. Zhou, N. J. Lin, M. T. Cicerone, C. L. Soles, S. Lin-Gibson, *Adv. Mater.* **2011**, *23*, 421.
[31] Y. Tsuda, T. Shimizu, M. Yamato, A. Kikuchi, T. Sasagawa, S. Sekiya, J. Kobayashi, G. Chen, T. Okano, *Biomaterials* **2007**, *28*, 4939.
[32] A. Chen, D. K. Lieu, L. Freschauf, V. Lew, H. Sharma, J. Wang, D. Nguyen, I. Karakikes, R. J. Hajjar, A. Gopinathan, E. Botvinick, C. C. Fowlkes, R. A. Li, M. Khine, *Adv. Mater.* **2011**, *23*, 5785.
[33] W. Liu, S. Thomopoulos, Y. Xia, *Adv. Healthcare Mater.* **2012**, *1*, 106.
[34] C. Mandoli, F. Pagliari, S. Pagliari, G. Forte, P. Di Nardo, S. Licoccia, E. Traversa, *Adv. Funct. Mater.* **2010**, *20*, 1617.
[35] N. Kachouie, Y. Du, H. Bae, M. Khabiry, A. F. Ahari, B. Zamanian, J. Fukuda, A. Khademhosseini. *Orgenogenesis* **2010**, *6*, 234.
[36] H. Tekin, G. Ozaydin-Ince, T. Tsinman, K. K. Gleason, R. Langer, A. Khademhosseini, M. C. Demirel, *Langmuir* **2011**, *27*, 5671.
[37] H. Aubin, J. W. Nichol, C. B. Huston, H. Bae, A. L. Sieminski, D. M. Cropek, P. Akhyari, A. Khademhosseini, *Biomaterials* **2010**, *31*, 6941.
[38] X. Shi, Y. Wang, L. Ren, W. Huang, D. A. Wang, *Int. J. Pharm.* **2009**, *373*, 85.
[39] J. Panyam, V. Labhasetwar, *Adv. Drug Delivery Rev.* **2003**, *55*, 329.
[40] A. Giteau, M. C. Venier-Julienne, A. Aubert-Poüssel, J. P. Benoit, *Int. J. Pharm.* **2008**, *350*, 14.
[41] S. H. Lee, H. Mok, Y. Lee, T. G. Park, *J. Controlled Release* **2011**, *152*, 152.
[42] K. Ren, W. Dai, J. Zhou, J. Su, H. Wu, *Proc. Natl. Acad. Sci. USA* **2011**, *108*, 8162.
[43] W. Dai, Y. Zheng, K. Q. Lou, H. Wu, *Biomicrofluidics* **2010**, *4*, 024101.
[44] E. J. Anglin, M. P. Schwartz, V. P. Ng, L. A. Perelman, M. J. Sailor, *Langmiur* **2004**, *20*, 11264.
[45] J. H. C. Wang, F. Jia, T. W. Gilbert, S. L. Y. Woo, *J. Biomech.* **2003**, *36*, 97.
[46] A. S. Andersson, P. Olsson, U. Lidberg, D. Sutherland, *Exp. Cell. Res.* **2003**, *288*, 177.
[47] A. M. Rajnicek, L. E. Foubister, C. D. McCaig, *Biomaterials* **2008**, *29*, 2082.
[48] E. M. Bouta, C.W. McCarthy, A. Keim, H. B. Wang, R. J. Gilbert, J. Goldman, *Acta Biomater.* **2011**, *7*, 1104.
[49] S. Oh, K. S. Brammer, Y. S. Li, D. Teng, A. J. Engler, S. Chien, S. Jin, *Proc. Natl. Acad. Sci. USA* **2009**, *106*, 2130.
[50] S. Watari, K. Hayashi, J. A. Wood, P. Russell, P. F. Nealey, C. J. Murphy, D. C. Genetos, *Biomaterials* **2012**, *33*, 128.
[51] D. C. Popescu, R. Lems, N. A. A. Rossi, C. T. Yeoh, J. Loos, N. A. J. M. Sommerdijk, *Adv. Mater.* **2005**, *17*, 2324.
[52] J. N. H. Shepherd, S. T. Parker, R. F. Shepherd, M. U. Gillette, J. A. Lewis, R. G. Nuzzo, *Adv. Funct. Mater.* **2011**, *21*, 47.
[53] M. J. Dalby, M. O. Riehle, S. J. Yarwood, C. D. W. Wilkinson, A. S. G. Curtis, *Exp. Cell Res.* **2003**, *284*, 274.
[54] C. Miller, S. Jeftinija, S. Mallapragada, *Tissue Eng.* **2001**, *7*, 705.
[55] W. Huang, Y. Wang, L. Ren, C. Du, X. T. Shi, *Mater. Sci. Eng. C* **2009**, *29*, 2221.
[56] J. S. Park, K. Park, D. G. Woo, H. N. Yang, H. Chung, K. Park, *Small* **2008**, *4*, 1950.
[57] X. Shi, H. Chang, S. Chen, C. Lai, A. Khademhosseini, H. Wu, *Adv. Funct. Mater.* **2012**, *22*, 751.
[58] Y. Wang, X. Shi, L. Ren, C. Wang, D. A. Wang, *Mater. Sci. Eng. C* **2009**, *29*, 2502.
[59] X. Shi, Y. Wang, R. R. Varshney, L. Ren, Y. Gong, D. A. Wang. *Eur. J. Pharm. Sci*. **2010**, *39*, 59.
[60] Y. Gong, K. Su, T. T. Lau, R. Zhou, D. A. Wang. *Tissue Eng. A* **2010**, *16*, 3611.